

**TO EMPLOY SOA-BASED OPTICAL SSB
MODULATION TECHNIQUE IN FULL-DUPLEX ROF
TRANSPORT SYSTEMS**

C.-L. Ying

Department of Electronic Engineering
Jinwen University of Science and Technology
Taipei 231, Taiwan, Republic of China

H.-H. Lu

Institute of Electro-Optical Engineering
National Taipei University of Technology
Taipei 106, Taiwan, Republic of China

W.-S. Tsai

Department of Electrical Engineering
Mingchi University of Technology
Taipei 243, Taiwan, Republic of China

H.-C. Peng and C.-H. Lee

Institute of Electro-Optical Engineering
National Taipei University of Technology
Taipei 106, Taiwan, Republic of China

Abstract—A full-duplex radio-over-fiber (ROF) transport system employing semiconductor optical amplifier (SOA)-based optical single sideband (SSB) modulation technique is proposed and demonstrated. For our proposed approach, it is relatively simple to implement as it requires only one SOA to generate optical SSB signal. Over an 80 km single-mode fiber (SMF) transmission, low bit error rate (BER), clear eye diagram, and low third-order intermodulation distortion to carrier ratio (IMD_3/C) were achieved. Our proposed full-duplex ROF transport systems are suitable for the long-haul microwave optical links.

Corresponding author: H.-H. Lu (hhlu@ntut.edu.tw).

1. INTRODUCTION

To meet the rapid growth for bit rate and bandwidth demands in communication systems, the convergence of wired and wireless networks is a promising solution. Radio-over-fiber (ROF), the integration of optical and wireless systems [1–4], is an attractive solution for increasing the transmission capacity and flexibility, as well as offering economic advantage due to its broad bandwidth and low attenuation characteristics. In general, the conventional optical double sideband (DSB) modulation technique is employed in ROF transport systems. However, transmitting the optical carrier and both sidebands is not the most efficient way to transmit information. Optical single sideband (SSB) modulation technique, which can remove a half of the optical spectrum, is expected to obtain a dispersion benefit since that the optical signal spectrum has been reduced by a factor of two [5]. With optical SSB modulation technique, RF power degradation due to fiber dispersion is reduced and thus the performances of systems are improved. In this paper, a full-duplex 70 Mbps/10 GHz (WiMAX compatible format) ROF transport system employing semiconductor optical amplifier (SOA)-based optical SSB modulation technique is proposed and demonstrated. The fixed WiMAX standard (IEEE 802.16d) specified WiMAX for the 2 to 11 GHz range, and it provides up to 70 Mbps speed. Several ways have been proposed to generate optical SSB signal. But, sophisticated sideband filtering and injection-locked techniques [6, 7], as well as expensive dual electrode Mach-Zehnder modulator (MZM) and phase modulator [8, 9] are required. However, a successful deployment of ROF transport systems strongly depends on the availability of simple architecture. This proposed approach is relatively simple to implement, as it requires only one SOA. Additional sophisticated techniques or expensive optical devices are not required. The feasibility of using SOA for generating optical SSB signal was demonstrated previously [10]. However, full-duplex ROF transport systems using SOA to generate optical SSB signal has not yet been reported. To the best of our knowledge, it is the first time to setup a full-duplex ROF transport system employing SOA-based optical SSB modulation technique. Over an-80 km single-mode fiber (SMF) transport both for down/up-link transmission, low bit error rate (BER), clear eye diagram, and low third-order intermodulation distortion to carrier ratio (IMD3/C) were obtained. We have experimentally demonstrated the feasibility of our proposed full-duplex ROF transport systems with compatible WiMAX format over a long-haul fiber link.

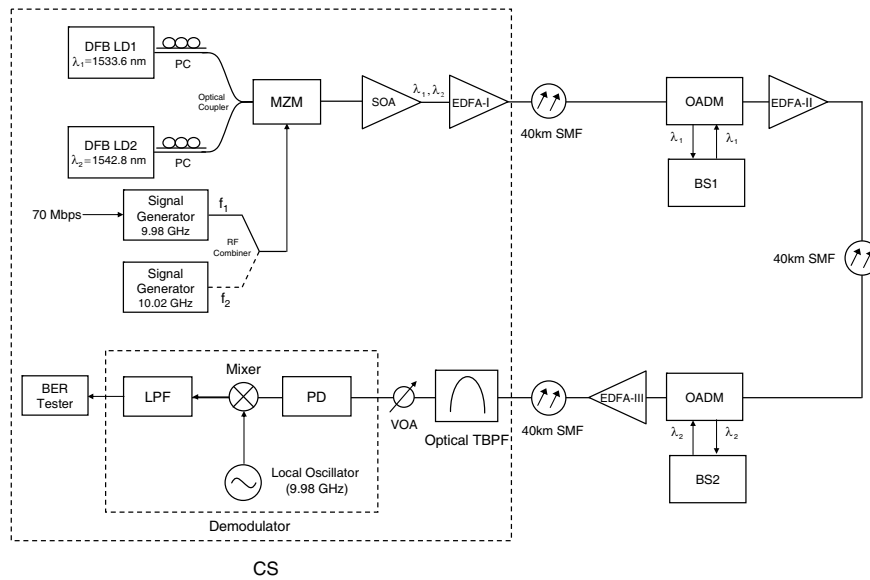


Figure 1. The experimental configuration of our proposed full-duplex ROF transport systems.

2. EXPERIMENTAL SETUP

Figure 1 shows the experimental configuration of our proposed full-duplex ROF transport systems employing SOA-based optical SSB modulation technique. For down-link transmission, the central station (CS) is composed of two distributed feedback laser diodes (DFB LDs), one MZM, one SOA, one erbium-doped fiber amplifier (EDFA), and two microwave signal generators. Between the two DFB LDs and the 2×1 optical coupler are the polarization controllers (PCs). The PCs are for polarization-dependent characteristic of MZM. The central wavelengths of these two DFB LDs are 1533.6 nm (λ_1) and 1542.8 nm (λ_2), respectively. Two DFB LDs provided two optical carriers to the MZM, and a low bias voltage was applied to the MZM. The optical signals of the MZM were coupled into the SOA to generate optical SSB signals.

70-Mbps data stream is mixed with microwave carrier ($f_1 = 9.98$ GHz) to generate the 70 Mbps/9.98 GHz binary phase-shift keying (BPSK) data signal. The resulting microwave data signal is then supplied to the MZM. The bandwidth of the MZM used in this experiment possesses a 3-dB cutoff frequency of 15 GHz, it means that 9.98 GHz microwave signal can be transmitted through the optical

links. At the CS, the optical signals are generated and then distributed through standard SMF to the remote base stations (BSs) (BS1 and BS2) by using cascaded EDFAs and optical add-drop multiplexers (OADMs). The optical signals are transmitted through three SMF spans ($40\text{ km} \times 3$) with the help of three EDFAs. Each BS is connected to the fiber backbone through an OADM which deals with an individual wavelength. The appropriate wavelengths are dropped by the OADM in BSs. The OADM, with >40 dB add/drop channel isolation, consists of one fiber Bragg grating (FBG) located between two optical circulators (OCs). The functions of OADM are to drop the down-link wavelength to the BS from the fiber backbone, and to add the up-link wavelength to the fiber backbone from the BS. The optical signal is modulated by 70 Mbps/9.98 GHz data signal through a MZM, and passed through an SOA to generate the optical SSB-modulated signal. The down-link data signal is adjusted by a variable optical attenuator (VOA), and detected by a broadband photodiode (PD) to convert optical signal into RF one. The 70 Mbps/9.98 GHz data signal is fed into a BER tester for BER analysis after demodulation. For up-link transmission, the 70 Mbps/9.98 GHz data signal is transmitted through SMF to the CS, passed through an optical tunable band-pass filter (TBPF) to select the desired wavelength, attenuated by a VOA, detected by a PD to convert optical signal into RF one, and provided to a demodulator. For demodulation part, RF and local oscillator (9.98 GHz) signals are applied to a mixer, the output of the mixer is put through a low-pass filter (LPF) to obtain the data stream (70 Mbps). Finally, 70-Mbps data stream is fed into a BER tester for BER analysis. As to the IMD_3/C value measurement, an additional microwave carrier ($f_2 = 10.02$ GHz) is added in CS to provide two-tone signal measurement. The IMD_3/C value is measured by using a spectrum analyzer.

3. EXPERIMENTAL RESULTS AND DISCUSSION

When many BSs are deployed in full-duplex ROF transport systems, all down-link wavelengths are employed within the wavelength range 1530–1550 nm (C-band). The optimum modulation performance will be achieved because the 15-GHz band MZM employed in this work exhibits an optimum modulation performance from 1530 to 1550 nm. The full-duplex ROF transport systems exploit the available bandwidth of 1530–1550 nm to address multiple BSs. However, there exists crosstalk between optical channels in wavelength-division-multiplexing (WDM)-ROF systems. Crosstalk for systems with channel spacing <4 nm is dominated by the cross-phase modulation

(XPM) interaction [11]. XPM interaction between optical channels will induce intolerable amounts of distortions in WDM-ROF systems, in which deteriorating the performances of systems. Thereby, for better performances, our proposed systems can exploit the available bandwidth of 1530–1550 nm to address maximum multiple BSs with 4 nm channel spacing.

Figure 2a shows the optical DSB-modulated signal (1533.6 nm, λ_1) in an optical spectrum analyzer (OSA) at the SOA input, both sidebands are 9.98 GHz (~ 0.08 nm) away from the optical carrier. Figures 2b and 2c show the optical SSB-modulated signals in an OSA at the SOA output. And further, Figure 2d shows the optical

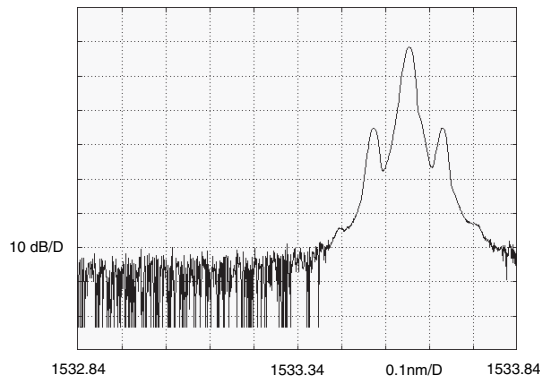


Figure 2a. The optical DSB-modulated signal (1533.6 nm, λ_1) at the SOA input.

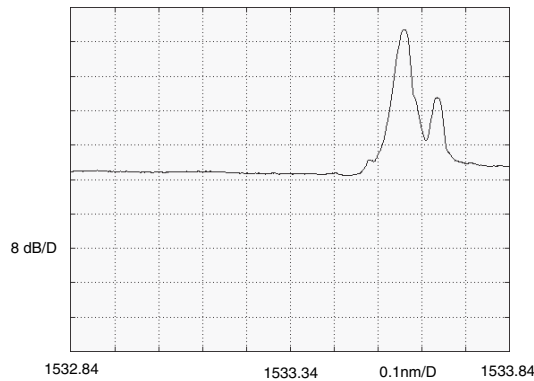


Figure 2b. The optical SSB-modulated signal in an OSA at the SOA output (SOA input optical power is -10 dBm per wavelength).

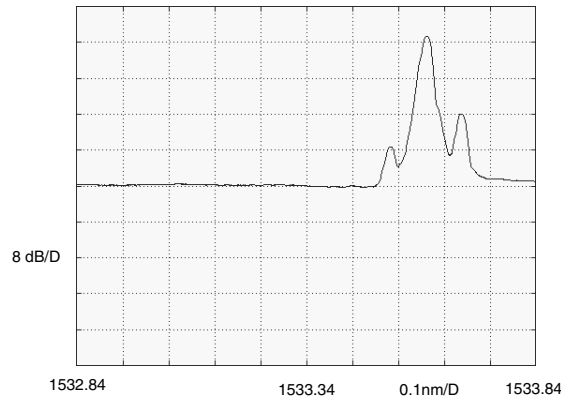


Figure 2c. The optical SSB-modulated signal in an OSA at the SOA output (SOA input optical power is -15 dBm per wavelength).

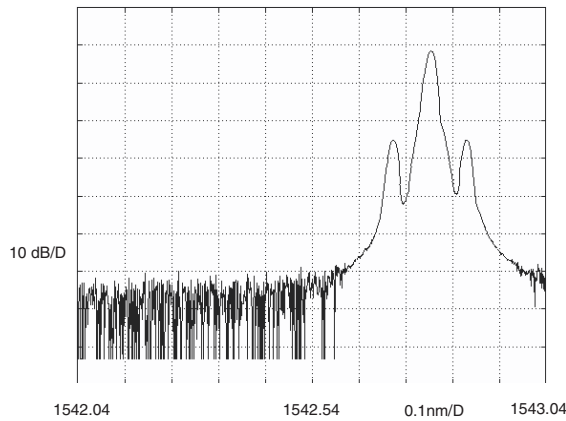


Figure 2d. The optical DSB-modulated signal (1542.8 nm, λ_2) at the SOA input.

DSB-modulated signal (1542.8 nm, λ_2) in an OSA at the SOA input. Figures 2e and 2f also show the optical SSB-modulated signals in an OSA at the SOA output. The optical SSB signal are obtained as the SOA input optical powers are -10 and -15 dBm per wavelength, respectively. When the optical DSB signal was coupled into the SOA at the input power of $-10 \sim -15$ dBm per wavelength, respectively. Moreover, since SOA is also employed at each BS to generate the optical SSB-modulated signal, thereby, the same performances for optical SSB-modulated signals at the SOA output can be obtained

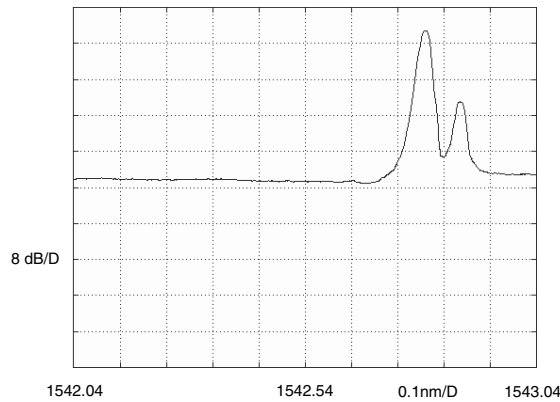


Figure 2e. The optical SSB-modulated signal in an OSA at the SOA output (SOA input optical power is -10 dBm per wavelength).

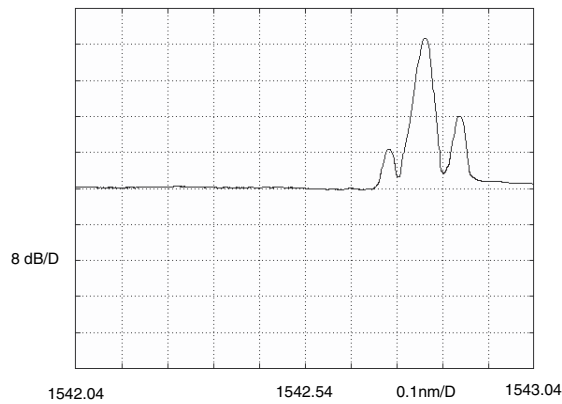


Figure 2f. The optical SSB-modulated signal in an OSA at the SOA output (SOA input optical power is -15 dBm per wavelength).

at each BS. When the optical DSB signal was coupled into the SOA at the input power of $-10 \sim -15$ dBm per wavelength, there was a large change in the optical signal at the SOA output. The amplitude of the optical sideband at the right-hand side of the optical carrier was not changed, but the amplitude of the optical sideband at the left-hand side of the optical carrier was suppressed, i.e., the optical SSB signal was created. In this proposed systems, optical SSB signal was created and transmitted as the SOA input optical power was -10 dBm per wavelength (λ_1 and λ_2).

Considering both self-phase modulation and self-gain modulation

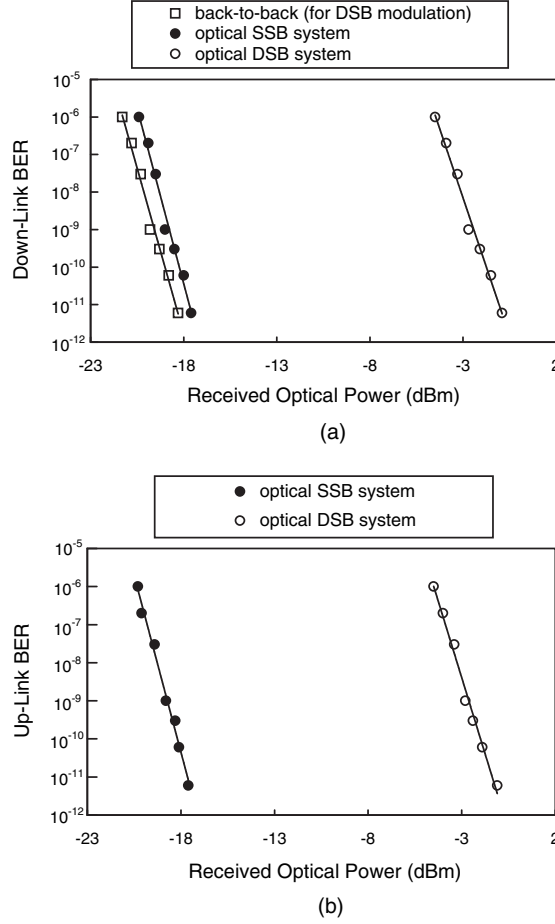


Figure 3. (a) The measured down-link BER curves of 70 Mbps/9.98 GHz data channel (CS \rightarrow BS2), (b) The measured up-link BER curves of 70 Mbps/9.98 GHz data channel (BS1 \rightarrow CS).

in the SOA, the electrical field of the output signal in an SOA can be expressed as [10]:

$$E(t) = E_0 \left[1 + \frac{m}{2} \sin(\omega_m t) \right] \cdot \exp \left[i\omega_0 t + (1 + i\alpha) \frac{m}{2} \eta P_{eff} \sin(\omega_m t + \beta) \right] \quad (1)$$

where E_0 is the output carrier amplitude, m is the input signal modulation index, ω_m is the subcarrier frequency, ω_0 is the optical carrier frequency, α is the linewidth enhancement factor, η is a coefficient that depends on the gain feature of the SOA, P_{eff} is the

Table 1. The power level differences between the carrier and the upper sideband for λ_1 at the SOA output at different input optical power per wavelength.

Input Optical Power (dBm)	Power Level Difference (dB)
-8	25.3
-9	26.2
-10	27
-11	26.5
-12	25.8
-13	25.2
-14	24.5
-15	24
-16	22.7
-17	21.4
-18	20

effective input optical power, and β is the phase difference between the change of carrier density and the change of input optical power. Expanding Equation (1) in Bessel series and neglecting high-order terms, the complex envelopes for the frequencies $\omega_0 + \omega_m$ (upper sideband) and $\omega_0 - \omega_m$ (lower sideband) can be estimated as:

$$E^{\omega_0 \pm \omega_m} \approx \mp \frac{im}{4} E_0 J_0(\chi) \cdot \{1 + \rho \exp[j(\theta \pm \beta)]\} \quad (2)$$

where $\theta = \tan^{-1} \alpha$, $\rho = \eta P_{eff} (1 + \alpha^2)^{1/2}$, and $\chi = \frac{-im\rho \exp(i\theta)}{2}$. Then sideband suppression ratio (SSR) can be derived:

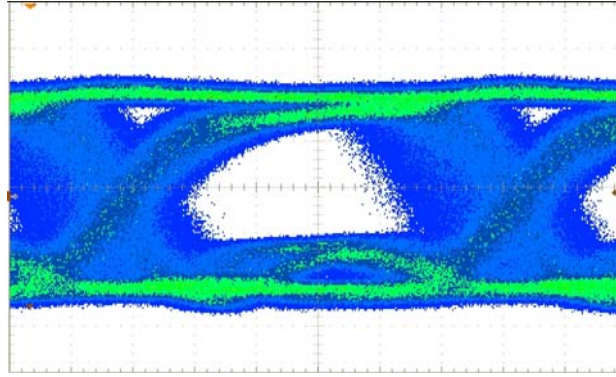
$$\text{SSR} = \left| \frac{E^{\omega_0 - \omega_m}}{E^{\omega_0 + \omega_m}} \right|^2 \approx \left| \frac{1 + \rho \exp[j(\theta - \beta)]}{1 - \rho \exp[j(\theta + \beta - \pi)]} \right|^2 \quad (3)$$

ρ is adjustable as a function of input optical power. Thereby, as $\rho \cos(\theta + \beta - \pi) = 1$, i.e., when

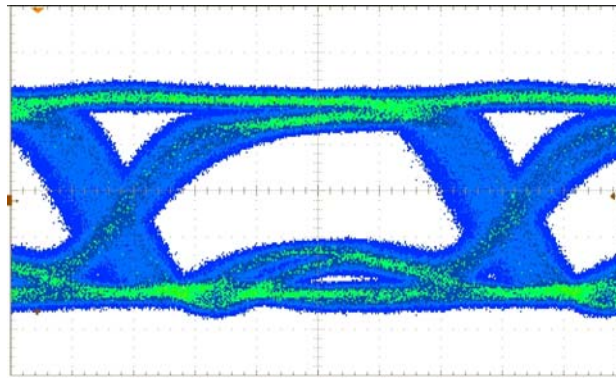
$$P_{eff} = (1 + \alpha^2)^{-1/2} \{ \eta \cos[\tan^{-1} \alpha - \tan^{-1}(\omega_m \tau_{eff})] \}^{-1} \quad (4)$$

The maximum SSR can be obtained. The power level differences between the carrier and the upper sideband for λ_1 at the SOA output at different input optical power per wavelength are given in Table 1. It

can be seen that the power level differences of 20~27 dB are achieved. As optimal optical powers are launched (-10 dBm per wavelength), the maximum power level difference of 27 dB is obtained. Under this condition, it corresponds with Equation (3) as denominator is approached to zero.



(a)



(b)

Figure 4. (a) The eye diagram of 70 Mbps/9.98 GHz data stream for optical DSB system, (b) The eye diagram of 70 Mbps/9.98 GHz data stream for optical SSB system.

The measured down-link BER curves of 70 Mbps/9.98 GHz data channel (CS \rightarrow BS2) are presented in Figure 3(a). At a BER of 10^{-9} ; for optical DSB system, the received optical power level is -2.7 dBm; for SOA-based optical SSB system, the received optical power level is -19 dBm. Receiver sensitivity improvement of 16.3 dB is obtained as SSB modulation technique is employed. And further,

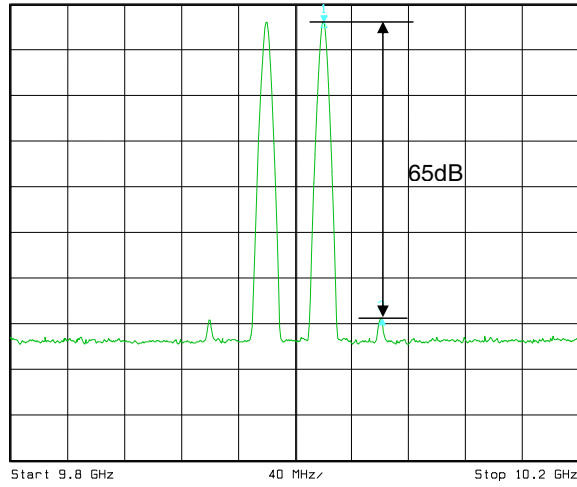


Figure 5. Electrical spectrum of the received signal with SOA-based optical SSB system.

the measured up-link BER curves of 70 Mbps/9.98 GHz data channel (BS1 \rightarrow CS) are presented in Figure 3(b). At a BER of 10^{-9} ; for optical DSB system, the received optical power level is -2.8 dBm; for SOA-based optical SSB system, the received optical power level is -18.8 dBm. Receiver sensitivity improvement of 16 dB is obtained as SSB modulation technique is employed. From Figure 3(a) we also can see that, at a BER of 10^{-9} , there exists a large power penalty of 17.1 dB between the back-to-back case (for DSB modulation) and the optical DSB system. But, at a BER of 10^{-9} , SOA-based optical SSB system exhibits a power penalty of only 0.8 dB. The BER is given by

$$BER = \frac{1}{2} \operatorname{erfc} \left(\sqrt{\frac{SNR}{2}} \right) \quad (5)$$

where SNR is systems' signal-to-noise ratio. Carrier power reduction will be reduced greatly as SOA-based optical SSB modulation technique is employed. The higher carrier power level we get, the higher SNR value we achieve. SOA-based optical SSB system increases the SNR value of system significantly, in which causing system with better BER performance, and leading to a large improvement of receiver sensitivity.

Figures 4(a) and (b) display the eye diagrams of 70 Mbps/9.98 GHz data stream (down-link: CS \rightarrow BS2) for optical DSB and SSB systems, respectively. Amplitude and jitter fluctuations are obviously observed

in optical DSB system (Figure 4(a)). DSB signal suffers fading problem due to fiber dispersion, in which resulting in the amplitude and jitter of eye diagram increase greatly. However, in SOA-based optical SSB system, clear eye diagram is obtained (Figure 4(b)). Electrical spectrum of the received signal with SOA-based optical SSB system is shown in Figure 5. It is obvious that the residue IMD_3/C level of -65 dBc or more is obtained. Carrier power degradation will be reduced as optical SSB modulation technique is employed, leading to an improvement of IMD_3/C value.

4. CONCLUSION

Full-duplex ROF transport systems employing SOA-based optical SSB modulation technique is proposed and demonstrated. Our proposed approach is relatively easy to implement, as it requires only one SOA to generate optical SSB signal. Over an-80 km SMF transmission, low BER, clear eye diagram, and low IMD_3/C were obtained. Our proposed full-duplex ROF transport systems are suitable for the long-haul microwave optical links.

REFERENCES

1. Serdyuk, V. M., "Dielectric study of bound water in grain at radio and microwave frequencies," *Progress In Electromagnetics Research*, PIER 84, 379–406, 2008.
2. Lin, C. T., J. Chen, P. C. Peng, C. F. Peng, W. R. Peng, B. S. Chiou, and S. Chi, "Hybrid optical access network integrating fiber-to-the-home and radio-over-fiber systems," *IEEE Photon. Technol. Lett.*, Vol. 19, 610–612, 2007.
3. Oraizi, H. and S. Hosseinzadeh, "A novel marching algorithm for radio wave propagation modeling over rough surfaces," *Progress In Electromagnetics Research*, PIER 57, 85–100, 2006.
4. Prat, J., M. C. Santos, and M. Omella, "Square root module to combat dispersion-induced nonlinear distortion in radio-over-fiber systems," *IEEE Photon. Technol. Lett.*, Vol. 18, 1928–1930, 2006.
5. Blais, S. R. and J. Yao, "Optical single sideband modulation using an ultranarrow dual-transmission-band fiber bragg grating," *IEEE Photon. Technol. Lett.*, Vol. 18, 2230–2232, 2006.
6. Lu, H. H., S. J. Tzeng, C. Y. Chen, and H. C. Peng, "CSO/CTB performances improvement by using optical SSB filter at the receiving site," *IEEE Trans. Commun.*, Vol. 53, 572–575, 2005.

7. Sung, H. K., E. K. Lau, and M. C. Wu, "Optical single sideband modulation using strong optical injection-locked semiconductor lasers," *IEEE Photon. Technol. Lett.*, Vol. 19, 1005–1007, 2007.
8. Smith, G. H., D. Novak, and Z. Ahmed, "Overcoming chromatic-dispersion effects in fiber-wireless systems incorporating external modulator," *IEEE Trans. Microwave Theory Tech.*, Vol. 45, 1410–1415, 1997.
9. Davies, B. and J. Conrad, "Hybrid modulator structure for subcarrier and harmonic subcarrier optical single sideband," *IEEE Photon. Technol. Lett.*, Vol. 10, 600–602, 1998.
10. Lee, U. S., H. D. Jung, and S. K. Han, "Optical single sideband signal generation using phase modulation of semiconductor optical amplifier," *IEEE Photon. Technol. Lett.*, Vol. 16, 1373–1375, 2004.
11. Lu, H. H., W. J. Wang, and W. S. Tsai, "CSO/CTB performances improvement in a bi-directional DWDM CATV system," *IEEE Trans. Broadcast.*, Vol. 50, 377–381, 2004.